TECHNICAL MEMORANDUM

515

Assimilation of MODIS cloud optical depths in the ECMWF model

A. Benedetti and M. Janisková

Research Department

To be submitted to *Monthly Weather Review*

April 2007

European Centre for Medium-Range Weather Forecasts
Europäisches Zentrum für mittelfristige Wettervorhersage
Centre européen pour les prévisions météorologiques à moyen terme

Series: ECMWF Technical Memoranda

A full list of ECMWF Publications can be found on our web site under:
http://www.ecmwf.int/publications/

Contact: library@ecmwf.int

European Centre for Medium-Range Weather Forecasts
Shinfield Park, Reading, RG2 9AX, England

Abstract

At the European Centre for Medium–Range Weather Forecasts (ECMWF), a large effort has recently been devoted to define and implement moist physics schemes for variational assimilation of rain and cloud–affected brightness temperatures. In this study we expand on the current application of the new linearized moist physics schemes to assimilate cloud optical depths retrieved from the Moderate Resolution Imaging Spectroradiometer (MODIS) on board of the Aqua platform, for the first time in the ECMWF operational four–dimensional assimilation system (4D–Var). Model optical depths are functions of ice water and liquid water contents through established parametrizations. Linearized cloud schemes in turn link these cloud variables with temperature and humidity. A bias correction is applied to the optical depths to allow for a better agreement of the differences between model and observations. The control variables in the assimilation are temperature, humidity, winds and surface pressure. One month assimilation experiments for April 2006 demonstrated an impact of the assimilated MODIS cloud optical depths on the model fields, particularly temperature and humidity. Comparison with independent observations indicate a positive effect of the cloud information assimilated into the model especially on the amount and distribution of the Ice Water Content. The impact of the cloud assimilation on the medium–range forecast is neutral–to–positive. Most importantly, this study demonstrate the feasibility of global assimilation of cloud observations in the context of a Numerical Weather Prediction system.

1. Introduction

The new frontier for improvement in weather forecasts and climate models from the point of view of defining the model initial state is the full use of avaliable satellite and ground–based data including cloud and precipitation–affected observations. Current satellite–based observations are rich in global cloud–related information. New sensors such as the Moderate Resolution Imaging Spectroradiometer (MODIS) on board of the Terra and Aqua satellites, the Cloud Profiling Radar (CPR) on board of CloudSat and the Cloud-Aerosol Lidar with Orthogonal Polarization (CALIOP) on board of CALIPSO, are revealing the complex two-dimensional and three–dimensional structures of clouds (Stephens et al., 2002). The challenge is now to extract the highest amount of information about the cloudy atmosphere from this wealth of data by using state-of-art modelling and assimilation systems.

The assimilation of cloud observations, using global Numerical Weather Prediction (NWP) systems, has been hampered by several factors: (i) the inherent nonlinearities and discontinuities in the cloud parametrization schemes, particularly those treating convection (Fillion and Mahfouf, 2003); (ii) the lack of suitable linearized cloud schemes for the minimization that could combine a description of the cloud fields close to the non-linear model with the computational efficiency of a linearized scheme, which is particularly important in an operational context (Janisková et al., 1999; Mahfouf, 1999); (iii) the complexity of the observation operators, e.g. the radiative transfer schemes for cloudy atmospheres especially in the presence of scattering (Greenwald et al., 2002, 2004; Matricardi, 2005); (iv) the definition of the bias for these observation operators; (v) the deviations from Gaussian distribution in the error statistics; and (vi) the difficulties in defining error background statistics for cloud control variables. Most of these problems are also common to the assimilation of rain–related measurements. The latter has received more attention in global NWP models (Županski and Mesinger, 1995; Tsuyuki, 1997; Bauer et al., 2006a,b, to mention a few studies), while cloud assimilation has been successfully implemented in limited–area models based on nudging technique (MacPherson et al., 1996; Lipton and Modica, 1999; Bayler et al., 2000), and mostly outside the operational context.

Initial cloud assimilation studies have focused on cloud retrievals from radar data, either in the context of one–dimensional variational schemes (Benedetti et al., 2003) or with fully–blown mesoscale models in 3D–Var (Hu et al., 2006a,b) and 4D–Var (Sun and Crook, 1998; Wung et al., 2000). Chevallier et al. (2004) investigated the capability of a 4D-Var system to assimilate cloud-affected satellite infrared radiances using observations

from the narrow-band Advanced Infrared Sounder (AIRS). An attempt at exploiting visible and infrared cloudy satellite radiances in 4D-Var variational assimilation has been made by Vukićević et al. (2004). In that study, the authors use the Regional Atmospheric Modeling and Data Assimilation System (RAMDAS) 4D–Var to estimate the cloud state from Geostationary Operational Environmental Satellite–9 (GOES–9) observations. Their findings show an improvement in the model cloud forecast, through enhanced vertical mixing and the coupling between initial conditions and observed state by the model dynamics. However, they also note that observations that are more directly related to local temperature and humidity are also needed to better constrain the system and reduce the errors. Lopez et al. (2006) also noted that in their 2D-Var assimilation of Atmospheric Radiation Measurement (ARM) cloud radar retrievals.

To-date a large percentage of satellite observations affected by clouds are not included in global analysis systems mainly because of the lack of suitable schemes to describe cloud processes in the assimilation with the necessary accuracy. Moist physics schemes for variational data assimilation that permit to treat complex cloud systems, while retaining the simplicity of being diagnostic and linearized, have been developed and are now operational in the European Centre for Medium–Range Weather Forecasts (ECMWF) 4D–Var system (Tompkins and Janisková, 2004; Lopez and Moreau, 2005). These developments have allowed the operational implementation of the 1D+4D–Var assimilation of rain and cloud–affected brightness temperatures from the Special Sensor Microwave/Imager (SSMI) (Bauer et al., 2006a,b). Results show a positive impact of these observations, especially in the redistribution of relative humidity in the Tropics, and consequently in the location of the precipitating systems. Despite this major achievement, a large percentage of the satellite data that are ingested in the ECMWF 4D-Var system is still screened for cloud and rain contamination, except for a few microwave and infrared channels whose sensitivity peaks in the upper troposphere/stratosphere. As a result, cloudy areas are still less constrained by observations than cloud–free areas.

In this study we attempt to demonstrate that the ECMWF 4D–Var system is technically ready to assimilate cloud observations. This is also thanks to the development of the new linearized moist physics schemes. As a first step, the visible cloud optical depths from the MODIS instrument on board of Aqua are used as observations. While it is recognized that dealing with the raw radiance measurements through the appropriate observation operators allows for a more consistent treatment of the observations within the model framework and a full utilization of the model sensitivity to observations (Vukićević et al., 2004; Moreau et al., 2004), the use of pre-processed cloud optical depths for testing purposes is more practical and less computationally demanding. Observational operators for visible radiances and their corresponding adjoints have been developed and applied in research contexts (Greenwald et al., 2002, 2004). However, in order to be used in an operational context, there is the need to make them efficient as it has been done over the years for infrared radiative transfer codes (Matricardi, 2005). It is envisaged that cloud retrievals will be replaced by the cloudy radiance observations for assimilation purposes, but for the time being the cloud retrievals represent a good, largely untapped, source of information on the cloud and the atmospheric state.

The outline of the paper is as follows. Section **2.** describes the general methodology and briefly provides details about the operational ECMWF 4D–Var system and the observation operators (cloud optical depth parametrizations and moist parametrization schemes). The main section, **3.**, describes the setup for one–month assimilation experiments with a brief introduction to the MODIS data and the discussion of the first–guess departures, of the bias correction and of the observation and representativeness errors. Section **4.** presents the outcome of the cloud assimilation experiment with respect to a reference run. Several measures of analysis performance are presented: from the standard assessment of an improved model fit to the assimilated observations to the validation against independent observations. The impact of the assimilation of cloud optical depth on key atmospheric parameters such as temperature, humidity and ice water content (IWC) is also shown. Some issues with the analysis of humidity are highlighted via comparisons with other assimilated observations which are sensitive to moisture. Section **5.** discusses the effect of the assimilation of cloud data on the medium–range forecast

using standard meteorological scores. The closing section, **6.**, summarizes the main findings and presents open questions and future perspectives of this line of work.

2. Methodology

a. The ECMWF operational 4D–Var

The ECMWF 4D–Var assimilation system is based on an incremental formulation which ensures a good compromise between operational feasibility and a physically consistent four–dimensional analysis (Courtier et al., 1994). The cost function in the incremental approach is formulated as follows:

$$\begin{aligned} \mathcal{J}(\delta\mathbf{x}_0) &= \mathcal{J}_b(\delta\mathbf{x}_0) + \mathcal{J}_o(\delta\mathbf{x}_0) + \mathcal{J}_c(\delta\mathbf{x}_0) \\ &= \frac{1}{2}(\delta\mathbf{x}_0)^T\mathbf{B}^{-1}(\delta\mathbf{x}_0) + \frac{1}{2}\sum_{i=0}^{n}\left(H'_i\delta\mathbf{x}_i - \mathbf{d}_i\right)^T\mathbf{R}_i^{-1}\left(H'_i\delta\mathbf{x}_i - \mathbf{d}_i\right) + \mathcal{J}_c(\delta\mathbf{x}_0) \end{aligned} \quad (1)$$

In this formulation, $\mathcal{J}_b(\delta\mathbf{x}_0)$ is the background cost function which measures the distance between the initial state of the model $\mathbf{x}_0$ and the background $\mathbf{x}_0^b$ obtained from a short-range forecast valid at the initial time of the assimilation period. $\mathcal{J}_o(\delta\mathbf{x}_0)$ is the observation cost function measuring the distance between the model trajectory and corresponding observations. A constraint cost function $\mathcal{J}_c(\delta\mathbf{x}_0)$ is used to include all the physical constraints one wants to impose on the model solution. In Eq. (1), $\delta\mathbf{x}_i = \mathbf{x}_i - \mathbf{x}_i^b$ is the analysis increment and represents the departure of the model state ($\mathbf{x}$) with respect to the background ($\mathbf{x}^b$) at any time t_i. H' is the linearized observation operator and $\mathbf{d}_i = \mathbf{y}_i^o - H_i(\mathbf{x}^b{}_i)$ is the departure of the model background equivalent from the observation ($\mathbf{y}_i^o$). The matrix $\mathbf{R}_i$ is the observation error covariance matrix, while $\mathbf{B}$ represents the background error covariance matrix, formulated according to the "wavelet–J_b" method of Fisher (2003; 2004). A nonlinear integration provides the linearization state - trajectory in the vicinity of which the model is linearized. The departures are computed during the nonlinear integration at high resolution using complex non-linear physics (as used by the forecast model).

Using the incremental approach, 4D-Var can be approximated to the first order as finding analysis increments $\delta\mathbf{x}_0^a$ which minimize the cost function $\mathcal{J}$. The minimization requires an estimation of the gradient of the cost function. The gradient with respect to $\delta\mathbf{x}_0$ is computed efficiently using the adjoint model. The minimization is solved using an iterative algorithm, based on the Lanczos conjugate gradient algorithm with appropriate preconditioning. In order to reduce the computational costs in the operational 4D–Var system, the perturbations $\delta\mathbf{x}_i$ are computed with a tangent-linear model using simplified physics (Mahfouf, 1999; Janisková et al., 2002; Tompkins and Janisková, 2004; Lopez and Moreau, 2005) at a lower resolution than the trajectory. The gradient of the cost function is computed with the low resolution adjoint model which also includes simplified physics. After the minimization, the trajectory and the departures are recomputed and a second minimization at a higher horizontal resolution is run. The model and observation operators are linearized again around the current state (Andersson et al., 2005; Radnóti et al., 2005). For this study we use a resolution of T511 (corresponding to approximately 40 km) for the forecast, while the two minimizations are run at T95 ($\sim$ 215 km) and T159 ($\sim$ 120 km). Moist physics are usually only activated in the second minimization, but in our configuration it was necessary to turn on the linearized moist physics schemes in both minimizations. On average, 50–70 iterations are required to reach a satisfactory convergence of the minimization. Convergence criteria and a detailed description of the incremental 4D–Var can be found in Fisher (1998) and Trémolet (2005).

The current assimilation window is 12 hours. Observations are ingested over the window and sub–divided into time slots of half hour. The model fields, including cloud liquid and ice water contents and cloud cover, required by the operators are interpolated at the observation location. This interpolation introduces a representativeness

error which increases the error variance of the observations. This component of the error should not be neglected and may be quite large for heterogeneous variables such as cloud fields. In this study we addressed this by artificially increasing the observation error as described in section **3.**f.. However, this is not an entirely satisfying solution. Recent efforts at ECMWF have shown that the representativeness error, in particular errors related to interpolation of non-homogenous fields such as precipitation and clouds to the observation locations can dominate the observation error (Philippe Lopez, private communication). An alternative to the interpolation would be a weighted nearest neighbour approach within a certain radius of distance between model grid-point and observation location. This approach is currently under development at ECMWF for the assimilation of rainy brightness temperatures and could be adapted to the assimilation of cloud–related observations.

b. Observational operators

The core of the observation operator for the cloud optical depth are the diagnostic linearized cloud scheme (Tompkins and Janisková, 2004) and the linearized convection scheme (Lopez and Moreau, 2005) providing detrained convective cloud water as input to the convective contribution of the cloud scheme. These schemes allow for a full representation of cloud systems in the context of the linearization approximations, and are tuned to match the full nonlinear parametrization schemes. The main advantage of the linearized schemes is the possibility to represent complex cloud and precipitation systems while retaining the computational efficiency which is required to run the several iterations during the minimization of the cost function. The schemes were first applied in the 1D+4D–Var assimilation of SSMI brightness temperatures and are currently fully operational in the ECMWF 4D–Var.

The main outputs of the linearized schemes, liquid water and ice water contents, are passed to the optical depth routine which computes the model equivalent of the observed optical depth at the observation location. This routine uses the Slingo (1989) parametrization for the optical properties of liquid water clouds and Fu (1996) for those of ice clouds. For liquid water clouds, the effective radius (r_e) is derived from the cloud liquid water content following Martin et al. (1994) with the concentration of cloud condensation nuclei fixed at 50 cm^{-3} over the oceans and 900 cm^{-3} over the continents. For ice clouds, the effective size of the particles is a function of temperature following Ou and Liou (1995).

Figure 1 illustrates the flow between the linearized moist parametrization schemes and the optical depth routines in 4D-Var computation. During the minimization, the linearized cloud scheme with input from the convection scheme provides the perturbations in cloud liquid and ice water content which are then passed to the tangent linear version of the optical depth routine to compute the perturbation of optical depth. In the backward calculation, the gradient of the cost function with respect to the control variables is calculated using first the adjoint of the optical depth routine to obtain the gradient with respect to the cloud liquid and ice water contents. The latter is then passed to the adjoint of the cloud and convection schemes and used to compute the cloud contribution to the gradient with respect to temperature and specific humidity, and through the convection scheme also to the gradient with respect to the wind components. The final gradient of the observation cost function with respect to the model state variables is transformed to the control–vector variables and passed together with the gradient of the background cost function to the minimization algorithm. Minimization provides the analysis increments $\delta\mathbf{x}_0^a$ to be added to the background $\mathbf{x}_0^b$ in order to obtain the model analysis.

As it can be seen from the flow diagram of Fig. 1, the control variables in the 4D–Var are temperature, humidity, vorticity, divergence and surface pressure. The cloud gradients computed by the adjoint of the moist parametrizations contribute directly to the gradients in temperature and humidity, and indirectly to the gradients in the other control variables, i.e. wind, through the coupling which takes place in the 4D–Var. Use of a moist control variable which cannot directly take into account the cloud increments is a major limitation of the current system. As a consequence the cloud–related observations can only impact the model indirectly and

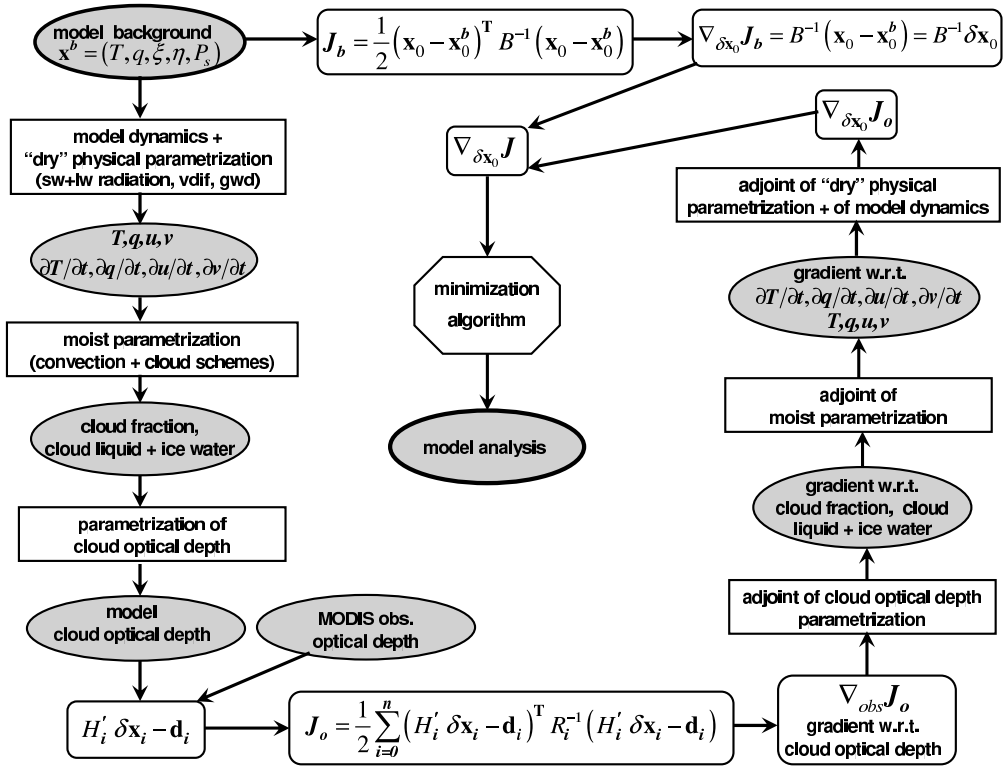

Figure 1: Flowchart describing the interaction between the linearized moist parametrization schemes and the optical depth scheme in the context of the standard 4D–Var minimization problem. See text for explanations.

in a way which is largely determined by the local, regime–dependent cloud Jacobians (Fillion and Mahfouf, 2003). Recognising this limitation, and to allow for a more effective assimilation of cloud observations, Sharpe (2006b,c) has implemented a total water control variable in the UK Met Office assimilation system. This variable is used to analyze moisture increments representing changes in total water substance defined as water vapor plus cloud liquid and ice water. More recently an incrementing operator for cloud fraction has also been included (Sharpe, 2006a). It is envisaged that a similar approach might be taken at ECMWF to increase the benefits of the assimilation of cloud–related observations, and improve background error statistics in cloudy and rainy areas.

3. Data and description of experimental setup

a. MODIS observations

The data used in this assimilation study is the cloud optical depth product from the MODIS instrument flying on board of Aqua. The cloud optical depth is retrieved from simultaneous cloud reflectance measurements in various solar spectral bands. Specifically, the water–absorbing bands (1.6, 2.1 and 3.7 μm) provide an estimate of the particle size while the non-absorbing bands (0.65, 0.86, and 1.2 μm) are chosen to minimize the effect of surface reflectance and mainly provide information on the visible optical thickness (Platnick et al., 2003; King et al., 2003). Most cloud level–2 products are provided at a resolution of 1 km. However, here we used the latest release, collection 5, that also provides a summary file which contains both cloud and aerosol retrieved

products at a resolution of 5 km at the standard reference wavelength of 0.55 μm (King et al., 2006). Before entering the assimilation, the MODIS cloud optical depth observations are further averaged to a resolution of 25km. This is done to minimize the mismatch between observations and model resolution (T511, approximately 40 km). The model equivalent optical depths are calculated at 0.55 μm using the observation operator described in the previous section.

b. Experimental setup

The experimental setup is similar to that of a former operational run at a resolution of T511. The incremental 4D–Var is initialized with a short forecast and all standard observations (conventional and satellite-based) are used in the minimization. During each 12-hour assimilation cycle, over three million observations that have passed the screening process are ingested in the 4D–Var. Some of this data is screened and/or thinned according to the system requirements. Since data acquisition for MODIS optical depth is not automated as it is for other observations, we processed only Aqua measurements for the month of April 2006. The data volume of these observations amounts to approximately one hundred thousand optical depth data points per cycle. A pre–screening is applied when the trajectory is run, and model optical depths smaller than 0.025 and larger than 100 are not included in the minimization as those are also the lower and upper limits, respectively, in the MODIS files. We also screen observations at high latitudes, i.e. above 60°, to avoid spurious optical depth retrievals over sea-ice. No further screening or thinning is applied to the averaged data. The minimization is run with the linearized moist physics in both the low (T95) and higher (T159) resolution inner loops. The cloud optical depths are included in the minimization via the Observational Data Base (ODB) as a special class of observations. All statistics about the first guess and analysis departures are collected in the ODB as for all other observations. The initial investigation was performed using the optical depth; it was then decided to assimilate instead the decimal logarithm of the optical depth to limit the range of increments and to obtain a more Gaussian distribution. Two sets of experiments were conducted with the logarithm cloud optical depth variable: one with and one without bias correction. Below is the rationale for these choices.

c. Logarithmic optical depth

One of the main underlying assumptions for a well-behaved variational assimilation is that of Gaussian error statistics for the background and observations errors as this implies that the cost function is quadratic and does not have multiple minima. This assumption translates into the requirement for a Gaussian distribution of the departures which represent the differences between the observations and their model equivalent. For variables such as precipitation and optical depth, however, it is observed that the departure statistics diverge from the Gaussian shape and are often skewed. The range of values that these departures can take is also wide, and that implies even larger deviations from "gaussianicity". Some authors suggest the use of change of variables to reduce the range of departures and improve their distribution. One of the most common choices for positive–definite variables, is to use the logarithm in decimal base of the model and observed quantities, as in Hou et al. (2004) for the assimilation of precipitation. Based on these considerations we decided to use this approach and develop the cloud assimilation in terms of logarithmic optical depth. Note that the errors on the logarithmic variables need also to be expressed in that form. Following Cohn (1997), we re–assigned errors on logarithmic optical depth according to the following formula:

$$r_{Log} = \sqrt{Log_{10}(1+\varepsilon_r^2)} \tag{2}$$

where r_{Log} is the error variance of the logarithmic optical depth and ε_r is the relative error on physical optical depth.

d. Monitoring of the first guess departures

When a new observation is introduced in the 4D–Var, a preliminary monitoring is performed by looking at the first guess departures which represent the difference between the observations and the model background in observation space. In an ideal system, the distribution of these departures should be centered around zero (unbiased model/observations) and Gaussian in shape. However the most likely scenario is that either the observations or the model, or both present biases. For the observations, the most common sources of bias are calibration errors of the instrument, scanning angle errors, and/or errors in the radiative transfer models that translate the atmospheric signal in radiances, which is what is measured by the space-borne instruments. All of the above sources of biases introduce biases in the retrieved cloud optical parameters. Model systematic errors are more difficult to describe as they can be due to a number of reasons ranging from inaccurate model parametrizations to errors introduced by the numerics. The weak–constraint 4D–Var addresses the problem of the inclusion of model error as part of the estimation problem (Trémolet, 2005). The discussion of this aspect of 4D–Var is, however, beyond the scope of the current study.

The assumption for the strong–constraint 4D–Var assimilation is that the first guess departures are unbiased, hence that diagonal elements of the observation error covariance matrix only describes the random component of the error. This is why a lot of effort is generally put toward either eliminating the biases at the preprocessing stage or in developing a bias model for the different sets of measurements that can be used to remove those biases in the 4D–Var context. This is the approach taken at ECMWF where a variational bias correction is implemented, and the coefficients describing the bias model are estimated as part of the minimization problem (Dee, 2004; Auligné et al., 2007). In our study, however, we could not make use of this method, as defining a bias model for cloud observations such as optical depth is not a trivial task. We then decided to run an experiment without bias correction and to investigate the first guess departure statistics with the purpose of modelling the optical depth bias. The first result that emerged was that observations over land had a much larger bias than the observations over ocean. This different behaviour could be due to the differences between the optical depth parametrization over land and over ocean. This aspect can be tested by choosing another set of parametrizations to see whether the bias is reduced, also by applying a tuning which is appropriate for the assimilation, and will be explored in future studies. As a first step, however, we decided to assimilate cloud optical depth observations over ocean only.

e. Bias correction

Figure 2a illustrates the nature of the bias problem. It shows the bias over ocean for over two million points accumulated during a two-week period (1-15 April 2006) from the monitoring run. As shown in the picture, the distribution of the first guess departures (i.e. the differences between observation and first guess) is not perfectly Gaussian (note the tail on the right hand side of the histogram) and the mean is not zero. It was decided to apply a simple bias correction as a function of the model optical depth in logarithmic space. The range of logarithmic optical depth (-1.6 to 2.0) was divided in eighteen bins and for each bin the average of the corresponding first guess departures was calculated. These averages were subsequently subtracted from the model optical depths falling in the specific bin. As a consequence the bias–corrected departures have a lower mean bias and the shape of their distribution is more Gaussian, as shown in Figure 2b. The bias as a function of optical depth is shown in Figure 3. Note that negative optical depths in logarithmic space are synonymous with optical depth smaller than unity in physical space. The shape of the bias curve is rather smooth. On average, the model has a positive bias for low optical depths, i.e it underestimates the cloud optical depth, whereas it has a negative bias for large optical depths, i.e. it overestimates the optical depth with respect to observations. In what follows, the term optical depth will signify logarithmic optical depth, unless otherwise stated.

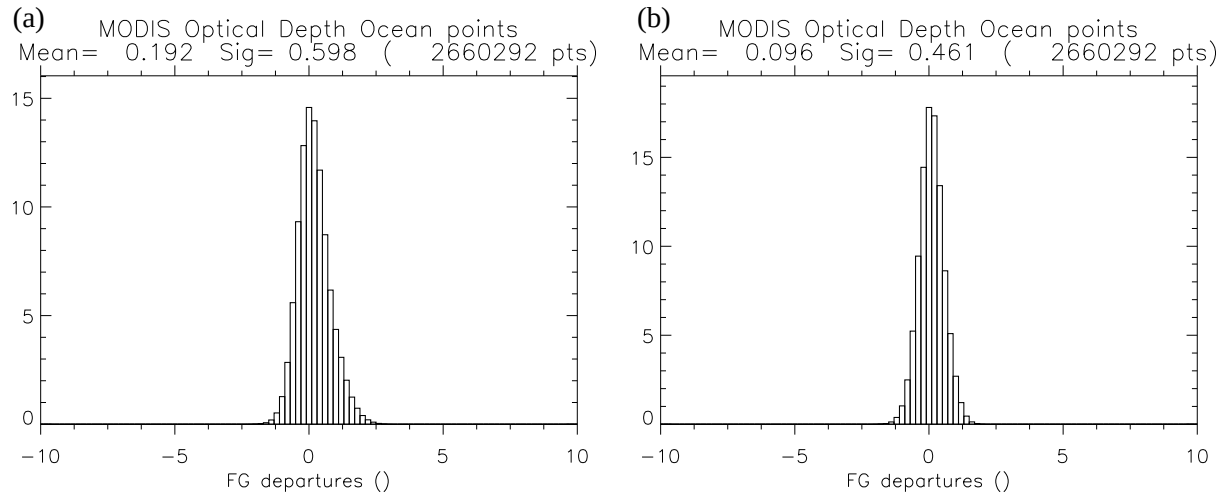

Figure 2: Probability distribution functions of first–guess departures in logarithmic optical depth (unitless): (a) before bias correction and (b) after bias correction.

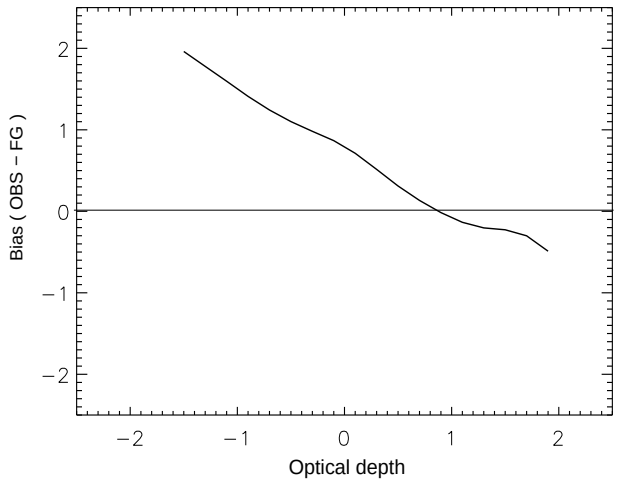

Figure 3: Bias in logarithmic optical depth as a function of the model logarithmic optical depth. See text for explanations.

f. Observation and representativeness errors

Although MODIS collection 5 cloud optical depths comes with a pixel–by–pixel uncertainty (King et al., 2006), initial assimilation tests were performed using an assumed value of 20% error on optical depth, translated using Eq. (2) into an error in logarithmic optical depth. This value was chosen as inclusive of various error sources such as the spectral albedo uncertainty (15%) and the calibration and radiative transfer model uncertainty (5%), as suggested in King et al. (2006). Additionally, the error was increased to 50% to partially account for representativeness errors deriving from the interpolation to observation location and those inherent to the optical depth observation operator and the parameters that describe it. For departures larger than 50 in physical space, an extra 50% for a total error of 100% was added to restrain the model within the assumptions of the incremental formulation, which assumes small departures from the model state. By doing so, large departures in optical depth are greatly penalized. We also increased to 150 % the error for retrieved values of optical depths greater

than 25 in an attempt to account for errors due to instrument saturation.

4. Assimilation results for April 2006

This section describes in detail the results for an assimilation run which included the bias correction for cloud optical depth. Various measures of the performance of the analysis are presented and discussed, including comparisons with independent observations.

a. Overview of the fit to observations

The first comparison that we made can be described as a sanity check: the analysed optical depths are plotted as a function of the observations and compared with the first–guess. In a successful analysis, the departures are smaller than in the first–guess, hence the analysis better matches the observations. Figure 4 shows scatterplots of first–guess and analysis plotted against observations. Due to the large data volume, to produce this figure we used only fifteen days in the middle of April. In panel (a) all data points are included in the first guess statistics, prior to the bias correction discussed in section **3.**e. Panel (b) shows the first guess statistics after application of the bias correction. It is possible to notice a large residual bias which indicates that the bias correction was not as effective as hoped for. This could be due to the fact that, when the number of first–guess optical depth values in a specific bin is low, the mean for that particular bin is not representative, hence a correction based on that estimated mean may not be suitable for all optical depth values. In fact, we can notice that the average bias represented by the black solid line in Fig. 4 is worse when the number of points in the optical depth interval is low (blue colours in the same figure). However, the total bias after the correction is 0.22 as opposed to a value of 0.35 prior to the correction. This indicates that the correction worked to a certain degree. Also Root Mean Square (RMS) error and correlation with observations are improved. This suggests that the simple bias correction which has been implemented is somehow effective in reducing systematic errors in the model optical depth. However, the persistence of the residual bias indicates that refinements to this correction are necessary. The analysis is shown in panel (c). The correlation with observations is much improved in the analysis. A small reduction in bias and RMS with respect to the first guess departures is also noticeable. However, these improvements in bias and RMS are small, consistently with the fact that the analysis is not supposed to correct for biases and confirming the need for a better *a priori* bias correction. Overall this scatterplot confirms that the analysis draws closer to the observations.

b. Impact of cloud assimilation on temperature, humidity and cloud parameters

In parallel with one month of cloud assimilation for April 2006, a reference run of the same length was also performed with an identical set–up to the cloud assimilation experiment, except for the use of MODIS data, to provide a benchmark for the impact of the introduction of cloud optical depths. Figure 5 shows the mean zonal differences between experiment and reference for temperature and specific humidity. These were averaged over the month of April and are shown as a function of pressure. The differences in specific humidity have a distinct vertical structure with a tendency for the experiment to be drier at upper and lower tropospheric levels and moister than the reference at middle levels across all latitudes up to $\pm 40^\circ$ S/N. Above this latitude, the prevalent pattern is that of larger moisture values in the experiment with respect to the reference. The pattern in temperature is more noisy but there is a distinct dipolar structure in the experiment of cooling at upper levels down to 750 hPa and warming below 750 hPa. Based on these impact plots, it appears that any changes induced by the cloud observations above 600 hPa reflect mainly a balance between a decrease in temperature which favours cloud formation and a reduction in specific humidity which opposes cloud formation. Between $\sim$600

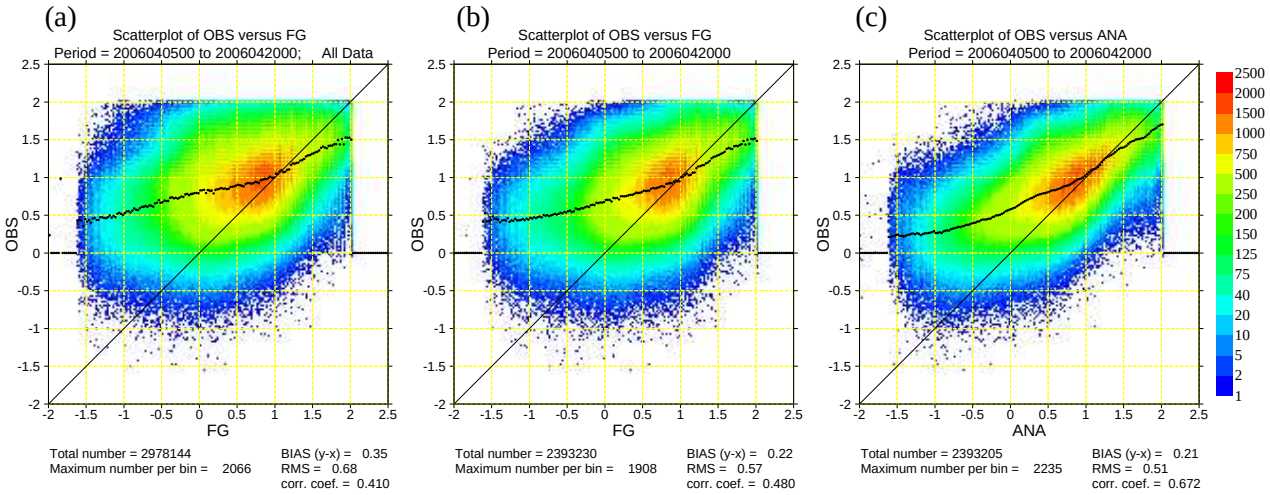

Figure 4: Scatterplot of (a) first–guess before applying bias correction, (b) first–guess after bias correction was applied and (c) analysis versus observations of logarithmic optical depth (unitless). The colour bar represents the population in each bin of logarithmic optical depth.

hPa and 750 hPa temperature and moisture changes seem to be more in phase as to enhance cloud formation, whereas at lower levels the situation is similar to that at upper levels.

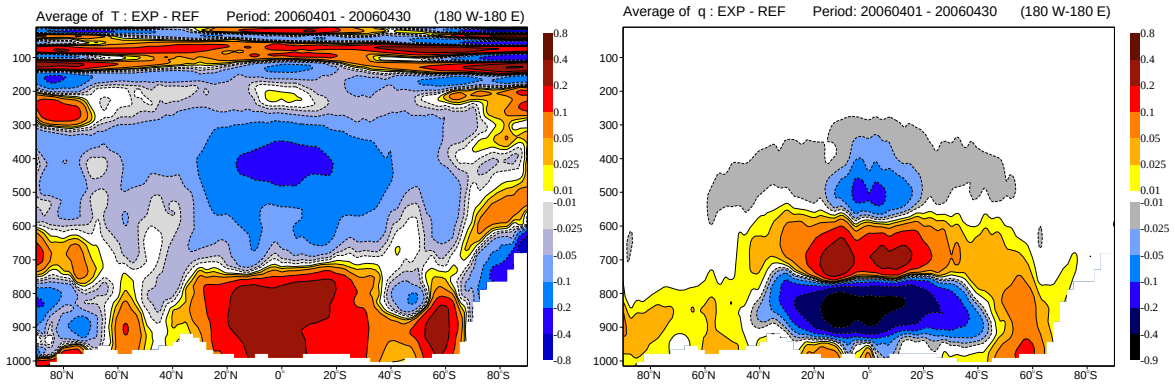

Figure 5: Zonal differences in temperature (K, left panel) and specific humidity (g/kg, right panel) between experimental and reference run averaged over the month and plotted as a function of pressure (hPa).

As a response to these changes in temperature and specifi c humidity in the analysis, there is a noticeable redistribution in Ice Water Path (IWP) and Liquid Water Path (LWP) at all latitudes which can be observed in the maps of monthly averages of the differences between experimental and reference run, shown in Fig. 6. Note especially the increase in LWP along the storm tracks and the decrease over the extra–tropical Pacifi c Ocean. IWP changes appear to have a more varied structure.

From these fi gures we can conclude that the assimilation of cloud optical depths has a large impact on the temperature, moisture and cloud fi elds. To ascertain whether this impact is positive, negative or neutral we compare both reference run and experiment with other assimilated observations in the 4D–Var or, when possible, with independent observations.

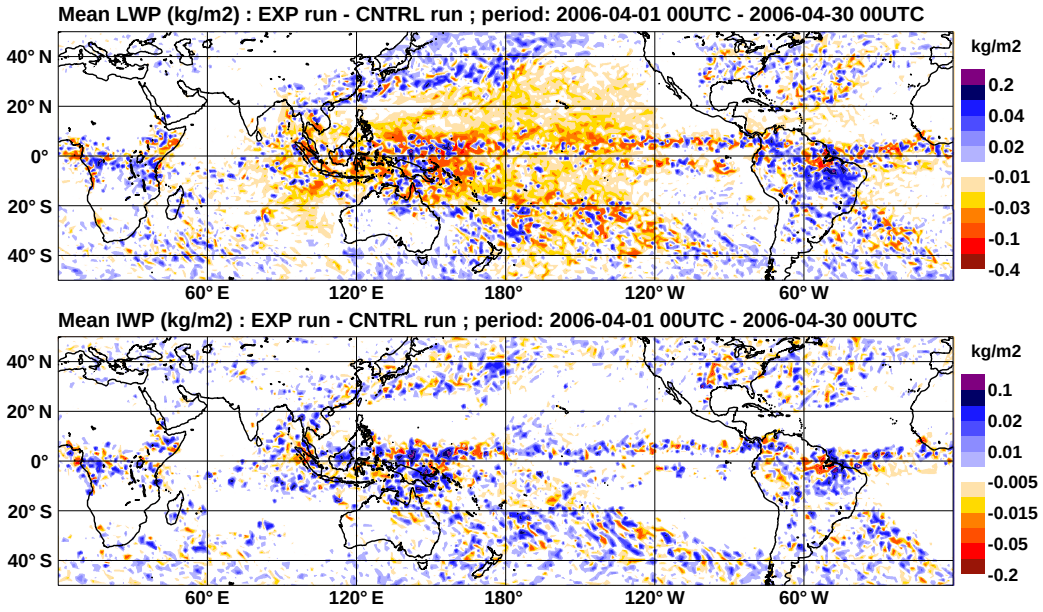

Figure 6: Horizontal maps of the differences in kg/m^2 of integrated liquid water path (top panel) and ice water path (lower panel) between experimental and reference run averaged over the month.

c. Comparisons with independent cloud observations

Comparisons in Ice Water Content (IWC) between the reference run and the experiment were carried out using independent data retrieved from the Microwave Limb Sounder (MLS) on board of Aura (Li et al., 2005, 2007). The MLS, operational since August 2004, has five radiometers measuring microwave emissions from the Earth's atmosphere in a limb-scanning configuration to retrieve chemical composition, water vapor, temperature and cloud ice. The retrieved parameters consist of vertical profiles on fixed pressure surfaces having near-global (82°N-82°S) coverage. The MLS IWCs are derived from cloud-induced radiances (CIR) using modelled CIR-IWC relations based on the MLS 240 GHz measurements. The IWCs have a vertical resolution of ∼3.5 km and a horizontal along-track resolution of ∼160 km for a single MLS measurement along an orbital track. This study uses MLS version 1.51 IWCs (Livesey et al., 2005) which are similar to the IWCs discussed in Li et al. (2005). In this version, the estimated precision for the IWC measurements is approximately 0.4, 1.0 and 4.0 mg/m^3 at 100, 147, and 215 hPa, respectively, which account for combined instrument plus algorithm uncertainties associated with a single observation.

Figure 7 shows a global map of the MLS IWC field at 215 hPa and the corresponding fields from the reference run and the cloud assimilation experiment. Percentage differences between MLS retrievals and model fields are also shown. From these it is possible to see qualitatively that the IWC from the cloud assimilation experiment is closer to the MLS observations than the reference run particularly over the equatorial West Pacific. In general assimilation of MODIS optical depths tends to reduce the values of 215 hPa IWC where these were high in the reference run. The signature of the Inter–Tropical Convergence Zone (ITCZ) is improved in the Atlantic and the Indian Ocean, and to a lesser extent over the Central Pacific.

This indicates that the cloud observations are effective in modifying the distribution of total tropospheric condensate in a manner that appears consistent with the MLS observations. Note for example the pattern of decrease in IWP at 5N over Indonesia in Fig. 6 where the reference run showed a moist bias in IWC at 215 hPa with respect to the MLS observations.

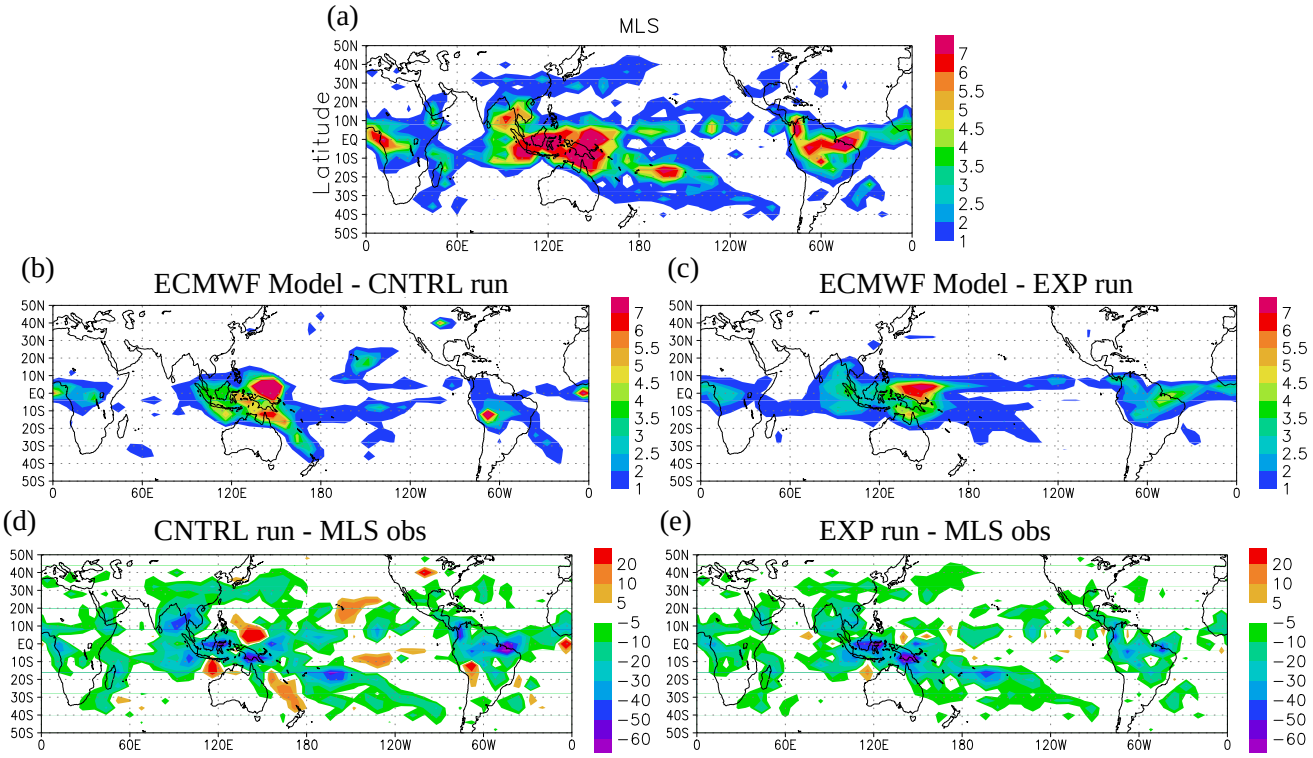

Figure 7: Maps of Ice Water Content at 215 hPa: MLS retrievals (top panel), reference run (left panel), and cloud assimilation experiment (right panel). Units of IWC are mg/m^3. The bottom panel shows the relative percent error with respect to the MLS retrievals of the reference run (left) and the cloud assimilation experiment (right), respectively. Plots were courtesy of Frank Li, Jet Propulsory Laboratory, CA, USA.

d. Comparisons with temperature and moisture–related observations

This section shows a series of plots that compare the reference and the experiment analyses with observations. The comparison focuses on the Tropics as this region appears to be greatly affected by the cloud assimilation (see impact plots of section **4.**b.). However similar trends are also seen for other regions.

Figure 8 shows statistics for Meteosat brightness temperature (Tb) observations over the Tropics in the water–vapor channel. These observations are not included in the minimization and can be considered as an independent source of validation for the first–guess and analysis. The shape of the first–guess and analysis departures for this Meteosat channel show a positive impact of the inclusion of cloud data. The mean of the first guess departures for the reference is 0.626 as opposed to 0.533 for the cloud assimilation experiment, indicating a better agreement of the background with the observations. For the analysis this mean value of departures is still lower for the cloud assimilation experiment (0.723 versus 0.806 for the reference). However, these mean values are larger than those of the first guess departures indicating a slight shift of both analyses from these observations that were not assimilated.

Figure 9 displays comparisons of the first guess (background) and analysis departures averaged over the whole month with respect to High Resolution Infrared Radiation Sounder (HIRS) Tb observations in the Tropics. These observations were included in the assimilation. Bias with respect to HIRS observations appear improved in the cloud assimilation experiment, particularly for channel 14 and 15. The bias correction applied to the observations and now estimated on–line in within the 4D–Var assimilation (Dee, 2004; Auligné et al., 2007) is

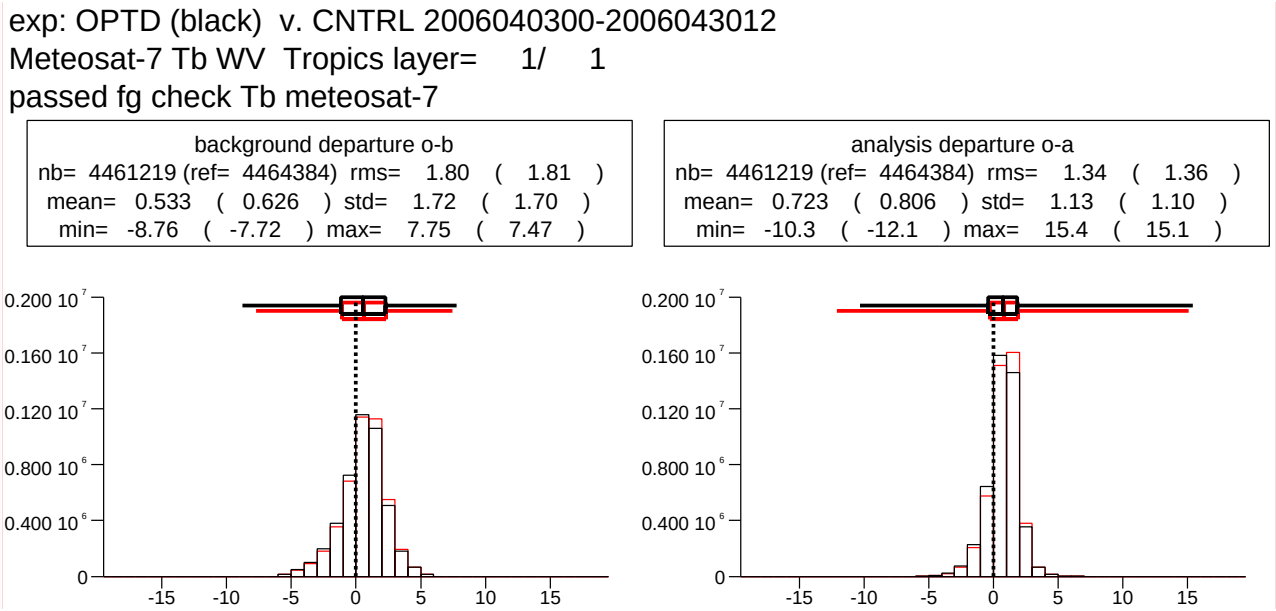

Figure 8: Statistics for Meteosat Tb observations in the water vapor channel over the Tropics. Reference run is in red and experiment in black. Left panel shows statistics for the background departure and right panel for the analysis departure. Statistical values are displayed for the reference run (in brackets) and for the experiment on the top of each panel.

also reduced for the cloud assimilation experiment with respect to the reference run (magenta and green dashed lines in the plot), indicating that the model confi guration with assimilated cloud data had a lower bias with respect to the HIRS observations. However, the standard deviation with respect to HIRS observations is not particularly improved in the humidity channels (11 and 12).

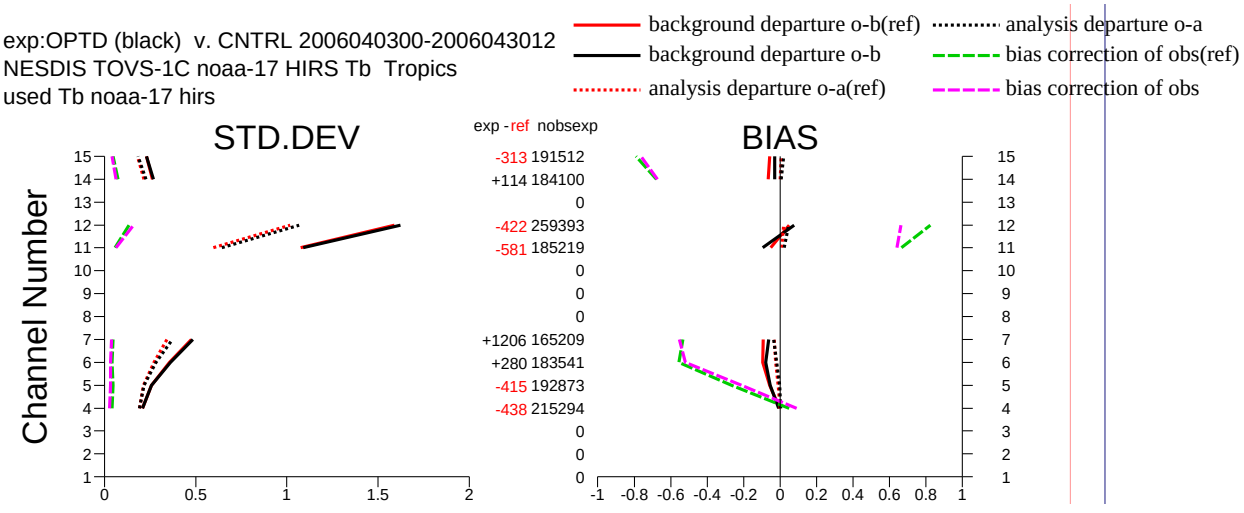

Figure 9: Standard deviation (left) and bias (right) of the background (solid line) and analysis (dashes line) departures from the HIRS brigthness temperature observations in the Tropics. Reference run is in red and experimental one in black. Magenta and green lines indicate the estimated bias correction for the HIRS observations for the cloud assimilation experiment and the reference run, respectively.

The adjustments in humidity induced by the cloud assimilation have an impact also on the clear–sky Tb which

provide information on the total column water vapor (TCWV). This impact is, however, not always positive as shown in Fig. 10. In this figure bias and standard deviation with respect to the Special Sensor Microwave Imager (SSM/I) clear–sky Tb observations in the Tropics are displayed. In this case, it is the reference run that performs slightly better than the cloud assimilation experiment and the standard deviation of the reference run is smaller than that of the cloud assimilation experiment. The bias correction for the observations is smaller in the reference for some channels, indicating an overall better agreement between observations and first guess. However, the two analyses are almost identical in terms of final bias. Comparisons with TCWV derived from rainy–affected SSMI Tb largely confirms the same behaviour.

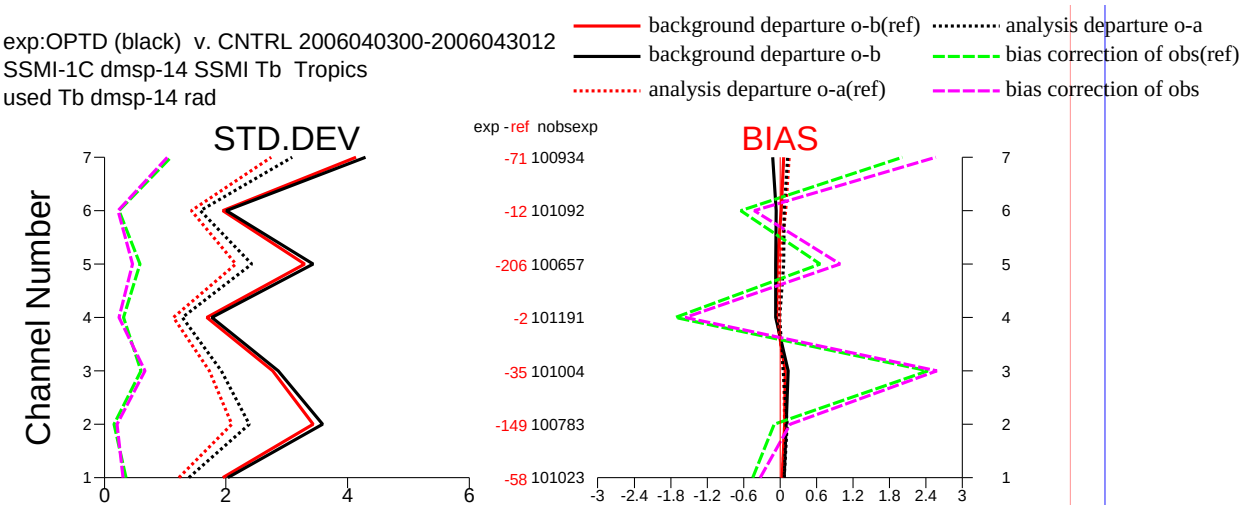

Figure 10: Same as Fig. 9, but for SSMI clear-sky Tb observations.

However, we observed that there are virtually no differences as far as it concerns bias and standard deviation between the reference and the experimental runs when considering a sensor which is more sensitive to temperature (e.g. Advanced Microwave Sounding Unit - AMSU-A).

The performance of two experiments is also compared in terms of relative humidity to radiosonde (TEMP) observations. Figure 11 shows bias and standard deviation of first guess and analysis for the control and the cloud assimilation experiment with respect to relative humidity based on temperature and humidity measurements. In this case a positive impact of the cloud observations can be noted, with a shift toward smaller negative biases at most levels for the cloud assimilation experiment. The analysis obtained from the experiment is also remarkably improved with respect to the reference run especially in the lower troposphere (1000 to 700 hPa). However, in terms of standard deviation the analysis from the cloud assimilation experiment performed worse than the reference run.

Overall these results show that the assimilation of cloud observations tends to affect the moisture balance in a slightly negative way. The assimilation experiment performs neutrally or worse than the reference run when compared with other assimilated observations from moisture–sensitive instruments, except for the positive impact shown in the comparison with the Meteosat data. The behaviour in temperature is mostly neutral.

5. Impact of the cloud assimilation on the forecast

The root mean square error, computed with respect to observations, is used as a measure to quantitatively compare the ten–day forecast from the reference run to that from the experiment which included cloud observations in the analysis. Figure 12 shows the mean RMS, averaged over the whole month of April, as a function of

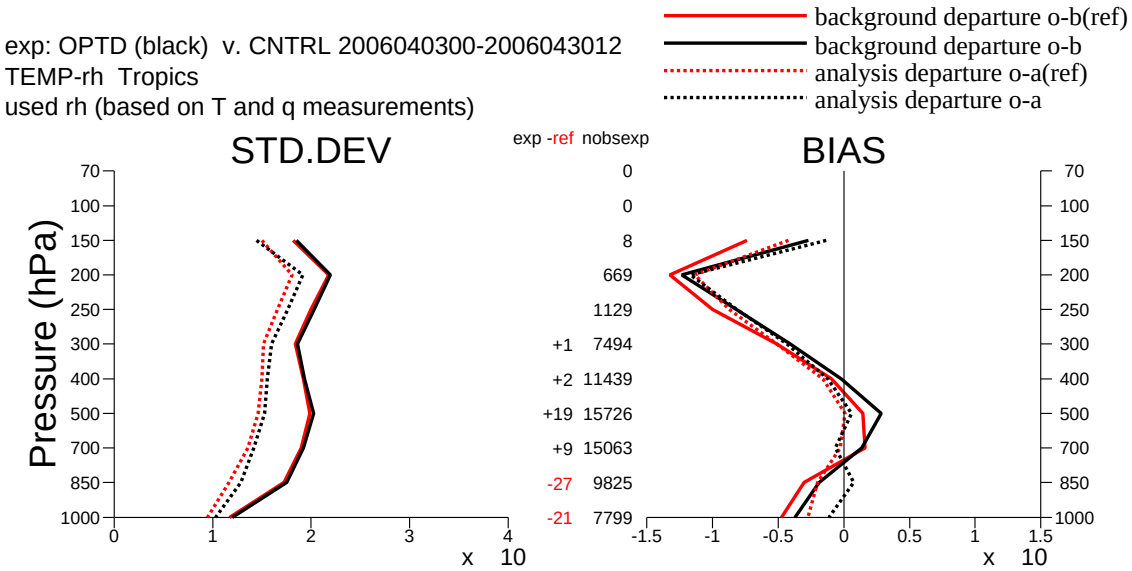

Figure 11: Same as Fig. 9, but for relative humidity based on TEMP temperature and humidity measurements.

forecast day for temperature at two levels, 850 and 500 hPa respectively, for Northern Hemisphere, Southern Hemisphere and Tropics. The impact of the assimilated cloud data on the Northern Hemispheric temperature is neutral with the two lines almost overlapping both at 850 and 500 hPa. For the Southern Hemisphere, the impact on temperature at 850 hPa is neutral up to forecast day 6. After that the control run shows a lower RMS than the cloud assimilation experiment. A similar behaviour is observed in the Tropics at 850 hPa with a slightly negative impact of the cloud assimilation on the forecasts. At 500 hPa and for short–term forecasts (day 1 to 4), the cloud assimilation experiment shows an overall lower RMS than the control.

A similar impact of the assimilated cloud data on the forecast is shown in Fig. 13, but this time for the wind variable at 850 and 700 hPa. The impact of the assimilation is neutral in the Northern Hemisphere, slightly positive in the Tropics and neutral to negative in the Southern Hemisphere.

Generally, the Tropics appear to be more influenced by the assimilation of cloud data than other areas, as already emphasized. The significance of this impact in the Tropics is shown in Figure 14 for temperature and wind RMS errors at the selected pressure levels over the period of 10 days. Statistical significance tells us how likely we would be to get differences between the groups that are being sampled (in our case difference between RMS errors of two different experiments) that are as large or larger than those we observe. The chosen confidence level 90% indicates that the probability of the observed behaviour being due to pure chance is less than 10% (or there is 90% chance of observed behaviour being true). The difference between two samples is computed as RMS of the reference run minus RMS of the experimental run, so a positive impact coming from the assimilation of cloud observations is marked by positive values, while the opposite is true for negative values. An inspection of the significance plots indicates that the impact of the cloud assimilation in the Tropics is positive, especially for temperature in the mid-troposphere at the beginning of the forecast period.

6. Discussion and conclusions

In this study, we used the ECMWF 4D–Var system to assimilate, for the first time on a global scale, MODIS cloud optical depth observations. The version of the 4D–Var included new linearized moist physics schemes that allow the treatment of cloud fields in the minimization. As the cloud variables are not part of the control vector, the increments which come from the cloud departures are translated into increments in temperature

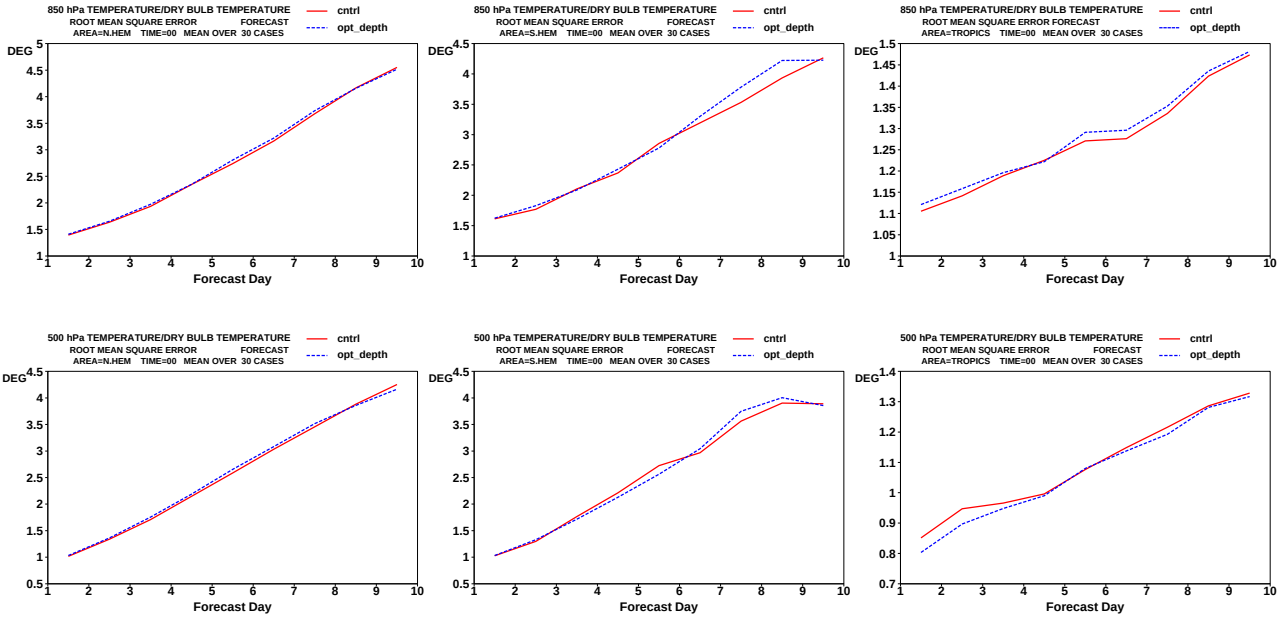

Figure 12: The RMS errors of 850 hPa temperature (top) and 500 hPa temperature (bottom) for a set of 30 forecasts compared to the observations. Control experiment based on the operational cycle (red solid line) and experiment with 4D-Var of cloud optical depth (blue dashed line). Areas shown are: Northern hemisphere (left), Southern hemisphere (middle) and Tropics (right).

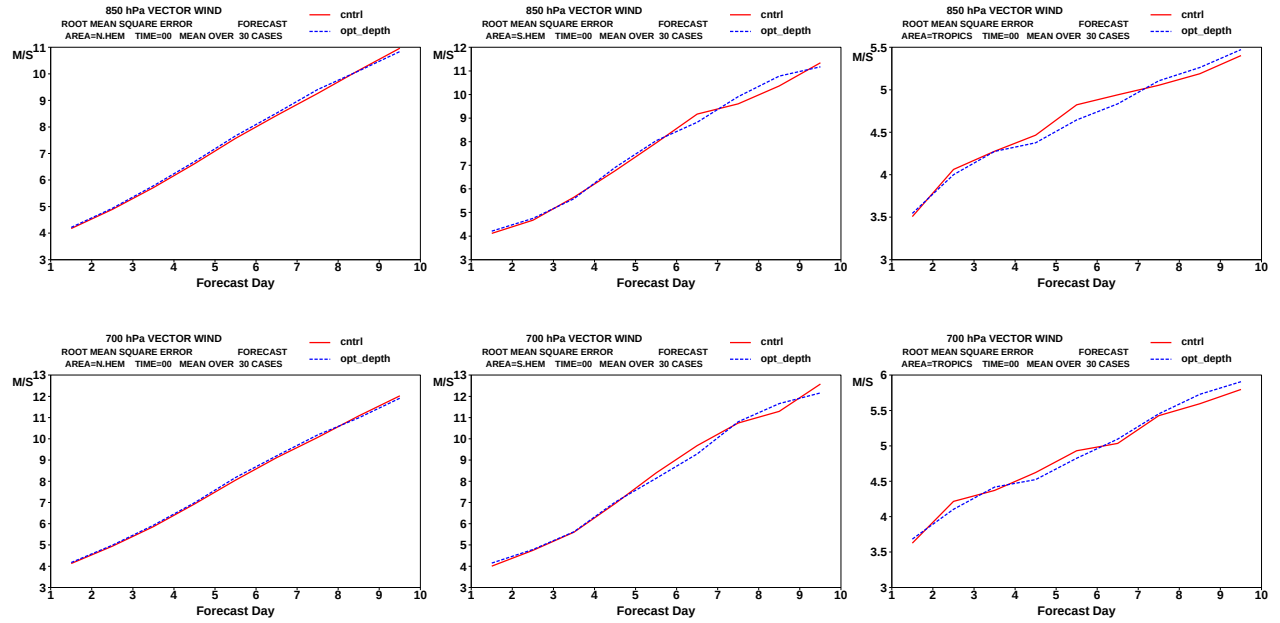

Figure 13: Same as Fig. 12, but for the RMS errors of 850 hPa and 700 hPa vector wind.

and specifi c humidity via the adjoints of the moist physics schemes. MODIS optical depths over ocean were added to the ECMWF observation database for the month of April 2006. Experiments were conducted to

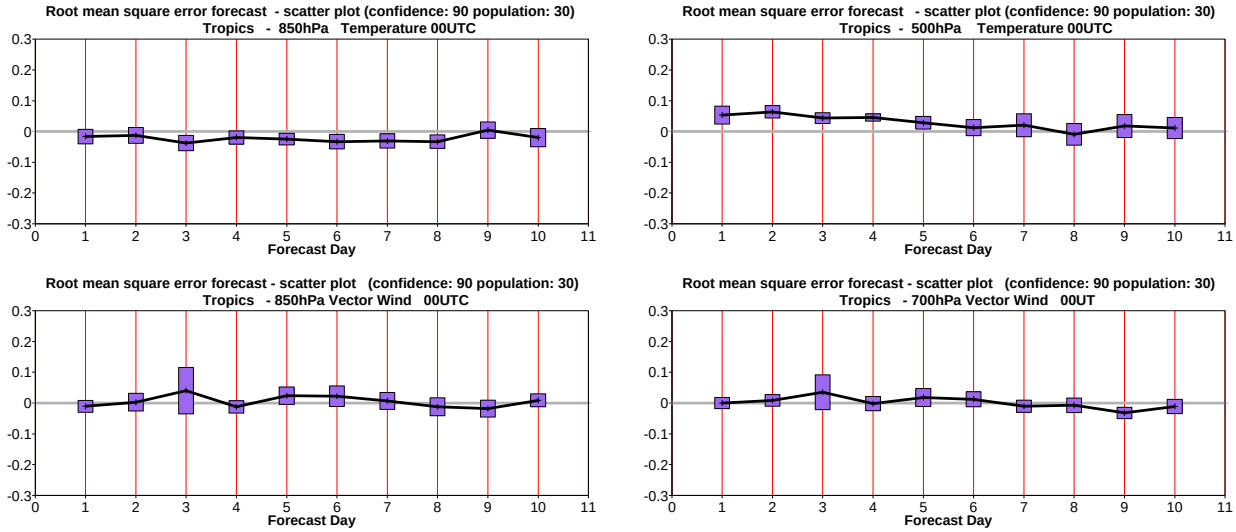

Figure 14: Significance of the impact coming from the assimilation of MODIS cloud optical depths in 4D-Var system for the period of April 2006 in the Tropics. The forecasts are compared with respect to the observations for 30 cases and significance is based on RMS error differences. Top panel shows the significance for 850 hPa and 500 hPa temperature, bottom panel for 850 hPa and 700 hPa vector wind.

assert the technical feasibility of the cloud assimilation, to monitor the optical depth bias in the ECMWF background fields and to find the most suitable model configuration for this type of exercise. A bias correction as a function of optical depth was implemented and a logarithmic variable was used to limit the range of optical depth departures. Results show that this bias correction worked only partially and needs to be revised in future studies. Despite the residual first–guess bias, the analysis is shown to draw closer to the observations and to improve the correlation between model and observed optical depth.

Results for the month of April 2006 show a positive impact of the cloud observations on the distribution of the Ice Water Content, particularly in the Tropics, as shown by comparisons with the Microwave Limb Sounder retrievals. However, comparisons with other assimilated observations show that the changes in specific humidity and TCWV induced by the assimilation of MODIS cloud optical depth retrievals, do not always improve the analysis fit to the observations. For sensors such as SSMI, the reference run performs noticeably better than the cloud assimilation experiment, indicating an imbalance in TCWV caused by the introduction of the cloud observations. The impact on temperature appears to be more neutral. This behaviour is not entirely inconsistent with the improvements in IWC described above. In fact, especially at the Tropics, at upper tropospheric levels, changes in the cloud fields can be achieved by small changes in temperature. Hence, even if the moisture field is affected in a slightly negative way, the cloud fields can still be more realistic when the cloud observations are assimilated due to temperature changes.

The impact of the cloud assimilation on the ten–day forecast as investigated using the RMS and the significance plots, appear to be positive for upper–level temperature in the Tropics, especially at the beginning of the forecast period. The impact is neutral for the model winds.

These results show that the ECMWF 4D–Var is approaching rapidly the level of technical maturity which is necessary for global assimilation of cloud related information, also thanks to the developments of efficient and accurate linearized moist parametrization schemes. Improvements in several areas are still necessary. For example, alternatives to the current interpolation method could ensure a better representativeness of the model cloud optical depths. At present, the cloud IWC and LWC are interpolated to the observations locations

as usually done in the operational data assimilation system. While this procedure might be satisfactory for more homogenous fields such as temperature, it might be less appropriate for cloud variables. Acknowledging this problem, an interpolation method for the assimilation of rainy radiances, which is based on weighing the contributions from all observations within a specific radius according to the distance from the model grid–point, is under investigation. This solution might also be beneficial for the cloud optical depth.

Improved parametrizations for the optical depth observation operator will allow better use of the data, especially over land. In the current study, it was found that the optical depth bias over land was larger than over ocean. It is known that cloud optical depth parametrizations take into account the fact that effective particle is larger and number concentration is smaller over ocean than over land due to the presence of fewer cloud condensation nuclei. To account for this, two sets of parameters for land and ocean are used in the cloud optical depth parametrization. These parameters could be still tuned to better match the observed optical depths. This could be addressed in a future study.

Developments in the inclusion of a total water variable in the control vector will also help in exploiting the information contained in the cloud observations. The current assimilation system uses humidity (in the form of normalized relative humidity - Hólm et al., 2002), temperature, surface pressure, vorticity and divergence as control variables. The linearized large–scale and convection schemes transfer increments derived from cloud observations into increments in the control variables. In this way, the contribution from cloud observations is included only indirectly in the 4D–Var. With the introduction of a total water variable, the link between cloud–related observations and control variables will become more direct, possibly avoiding problems in the redistribution of moisture increments between saturated and sub–saturated regions and hence improving the impact of the cloud data.

Furthermore, the use of weak–constraint 4D–Var to account for model systematic errors could also help with the problems emphasized in the changes in moisture induced by the cloud observations. At present the model is assumed to be error–free and in the context of the incremental 4D–Var only small departures from the model state are allowed (Andersson et al., 2005). Moreover, the whole 4D–Var system is somewhat "tuned" to clear–sky observations which represent the vast majority of observations integrated in the assimilation. When cloud observations are introduced the balance in the model background is perturbed and large increments in the control variables might occur. However, since there is no inclusion of model error, the system is not designed to deal with these large departures which are in contrast with the underlying assumption of the incremental 4D–Var. The lack of treatment of model error in the 4D–Var is highlighted by the introduction cloud observations as the model error is more likely to be larger for this type of model fields rather than more homogenous fields such as temperature and specific humidity. For these reasons, the full benefits of cloud assimilation will be more likely realized within a weak–constraint 4D–Var system.

Improvements notwithstanding, this study demonstrate the feasibility of global cloud assimilation in a numerical weather prediction model. The technical developments described in this paper pave the way for future assimilation of cloudy radiances which, in turn, will allow a more comprehensive exploitation of satellite data.

7. Acknowledgements

Thanks to Philippe Lopez and Jean-Jacques Morcrette (ECMWF) for their invaluable contribution in the process of this study. Peter Bauer and Erik Andersson are acknowledged for providing suggestions for improvement of earlier versions of the manuscript. Many thanks also to Duane Waliser and Frank Li (Jet Propulsory Laboratory, USA) that provided the comparison plots for the MLS data. The monitoring plots were kindly provided by Gerald Van der Grijn (ECMWF). We would like also to acknowledge Steve Platnick (NASA) for his help with MODIS data. Data for MODIS optical depth collection 5 were downloaded from the LAADS distribution site http://ladsweb.nascom.nasa.gov

References

Andersson, ., M. Fisher, E. Hólm, L. Isaksen, G. Radnóti, and Y. Trémolet, 2005: Will the 4D-Var approach be defeated by nonlinearity?, ECMWF Technical Memorandum No. 479.

Auligné, T., A. P. McNally, and D. Dee, 2007: Adaptive bias correction for satellite data in a numerical weather prediction system, *Q. J. R. Meteorol. Soc.*, accepted for publication.

Bauer, P., P. Lopez, A. Benedetti, D. Salmond, and E. Moreau, 2006a: Implementation of 1D+4D-Var assimilation of precipitation–affected microwave radiances at ECMWF. I: 1D-Var, *Q. J. R. Meteorol. Soc.*, **132**, 2277–2306.

Bauer, P., P. Lopez, D. Salmond, A. Benedetti, S. Saarinen, and M. Bonazzola, 2006b: Implementation of 1D+4D-Var assimilation of precipitation–affected microwave radiances at ECMWF. II: 4D-Var, *Q. J. R. Meteorol. Soc.*, **132**, 2307–2332.

Bayler, G. M., R. Aune, and W. H. Raymond, 2000: NWP cloud initialization using GOES sounder data and improved modeling of nonprecipitating clouds, *Mon. Weather Rev.*, **128**, 3911–3920.

Benedetti, A., G. L. Stephens, and T. Vukićević, 2003: Variational assimilation of radar reflectivities in a cirrus model. Part I: model description and adjoint sensitivity studies, *Quart. J. Roy. Meteor. Soc.*, **129**, 277–300.

Chevallier, F., P. Lopez, A. M. Tompkins, M. Janisková, and E. Moreau, 2004: The capability of 4D-Var systems to assimilate cloud-affected satellite infrared radiances, *Q. J. R. Meteorol. Soc.*, **130**, 917–932.

Cohn, S. E., 1997: An introduction to estimation theory, *J. Met. Soc. Jpn*, **75**, 257–288.

Courtier, P., J.-N. Thépaut, and A. Hollingsworth, 1994: A strategy for operational implementation of 4D–Var, using an incremental approach, *Q. J. R. Meteor.Soc.*, **120**, 1367–1387.

Dee, D., 2004: Variational bias correction of radiance data in the ECMWF system., Pp.97-112 in Proceedings of the ECMWF Workshop on Assimilation of high spectral resolution sounders in NWP, 28 June - 1 July 2004.

Fillion, J.-L. and J.-F. Mahfouf, 2003: Jacobians of an operational prognostic cloud scheme, *Mon. Weather Rev.*, **131**, 2838–2856.

Fisher, M., 1998: Minimization algorithms for variational data assimilation, In Seminar on Recent developments in numerical methods for atmospheric modelling. ECMWF, pages 364-385. September 1998.

Fisher, M., 2003: Background error covariance modelling, Shinfi eld Park, Reading, UK, pp. 45–64, Seminar on Recent developments in data assimilation for atmosphere and ocean, Reading, UK, 8-12 September 2003.

Fisher, M., 2004: Generalized frames on the sphere, with application to background error covariance modelling, Shinfi eld Park, Reading, UK, pp. 87–101, Recent developments in numerical methods for atmospheric and ocean modelling, 6-10 September 2004.

Fu, Q., 1996: An accurate parameterization of the solar radiative properties of cirrus clouds for climate models, *J. Climate*, **9**, 2058–2082.

Greenwald, T. J., R. Hertenstein, and T. Vukićević, 2002: An all-weather observational operator for radiance data assimilation with mesoscale forecast models, *Mon. Weather Rev.*, **130**, 1882–1897.

Greenwald, T. J., T. Vukićević, and L. D. Grasso, 2004: Adjoint sensitivity analysis of an observational operator for cloudy visible and infrared radiance assimilation, *Q. J. R. Meteorol. Soc.*, **130**, 685–705.

Hólm, E., E. Andersson, A. Beljaars, P. Lopez, J.-F. Mahfouf, A. J. Simmons, and J.-N. Thépaut, 2002: Assimilation and Modelling of the Hydrological Cycle: ECMWF's Status and Plans, ECMWF Technical Memorandum No. 383.

Hou, A. Y., S. Q. Zhang, and O. Reale, 2004: Variational continous assimilation of TMI and SSM/I rain rates: Impact on GEOS–3 hurricane analysis and forecast, *Mon. Weather Rev.*, **132**, 2094–2109.

Hu, M., M. Xue, and K. Brewster, 2006a: 3DVAR and Cloud Analysis with WSR-88D Level-II Data for the Prediction of the Fort Worth, Texas, Tornadic Thunderstorms. Part I: Cloud Analysis and Its Impact, *Mon. Wea. Rev.*, **134**, 675–698.

Hu, M., M. Xue, J. Gao, and K. Brewster, 2006b: 3DVAR and Cloud Analysis with WSR-88D Level-II Data for the Prediction of the Fort Worth, Texas, Tornadic Thunderstorms. Part II: Impact of Radial Velocity Analysis via 3DVAR, *Mon. Wea. Rev.*, **134**, 699–721.

Janisková, M., J.-J. M. J.-F. Mahfouf, and F. Chevallier, 2002: Linearized radiation and cloud schemes in the ecmwf model: Development and evaluation, *Q. J. R. Meteorol. Soc.*, **128**, 1505–1527.

Janisková, M., J.-N. Thépaut, and J.-F. Geleyn, 1999: Simplified and regular physical parameterizations for incremental four-dimensional variational assimilation, *Mon. Wea. Rev.*, **127**, 26–45.

King, M. D., W. P. Menzel, Y. J. Kaufman, D. Tanré, B.-C. Gao, S. Platnick, S. A. Ackerman, L. A. Remer, R. Pincus, and P. A. Hubanks, 2003: Cloud and Aerosol Properties, Precipitable Water, and Profiles of Temperature and Water Vapor from MODIS, *IEEE Trans. Geosci. Remote Sensing*, **41**, 442–458.

King, M. D., S. Platnick, P. A. Hubanks, G. T. Arnold, E. G. Moody, G. Wind, and B. Wind, 2006: Collection 005 Change Summary for the MODIS Cloud Optical Property (06_OD) Algorithm, Available at http://modis-atmos.gsfc.nasa.gov/C005_Changes/C005_CloudOpticalProperties_ver311.pdf. 23 pp.

Li, J.-L., J. H. Jiang, D. E. Waliser, and A. M. Tompkins, 2007: Assessing consistency between EOS MLS and ECMWF analyzed and forecast estimates of cloud ice, *Geophys. Res. Letters*, accepted for publication.

Li, J.-L., D. E. Waliser, J. H. Jiang, D. L. Wu, W. Read, J. W. Waters, A. M. Tompkins, L. J. Donner, J.-D. Chern, W.-K. Tao, R. A. aand Y. Gu, K. N. Liou, A. Del Genio, M. Khairoutdinov, and A. Gettelman, 2005: Comparisons of EOS MLS cloud ice measurements with ECMWF analyses and GCM simulations: initial results, *Geophys. Res. Letters*, **32**, doi: 10.1029/2005GL023788.

Lipton, A. E. and G. D. Modica, 1999: Assimilation of visible-band satellite data for mesoscale forecasting in cloudy conditions, *Mon. Weather Rev.*, **127**, 265–278.

Lopez, P., A. Benedetti, P. Bauer, M. Janisková, and M. Köhler, 2006: Experimental 2D-Var assimilation of ARM cloud and precipitation observations, *Q. J. R. Meteorol. Soc.*, **132**, 1325–1347.

Lopez, P. and E. Moreau, 2005: A convection scheme for data assimilation: Description and initial tests, *Q. J. R. Meteorol. Soc.*, **131**, 409–436.

MacPherson, B., B. J. Wright, W. H. Hand, and A. J. Maycock, 1996: The impact of MOPS moisture data in the U.K. Meteorological Office mesoscale data assimilation scheme, *Q. J. R. Meteorol. Soc.*, **124**, 1746–1766.

Mahfouf, J.-F., 1999: Influence of physical processes on the tangent–linear approximation, *Tellus*, **51**, 147–166.

Martin, G. M., W. Johnson, and A. Spice, 1994: The measurement and parameterization of of effective radius of droplets in warm stratocumulus, *J. Atmos. Sci.*, **51**, 1823–1842.

Matricardi, M., 2005: The inclusion of aerosols and clouds in RTIASI, the ECMWF fast radiative transfer model for the infrared atmospheric sounding interferometer, ECMWF Technical Memorandum No. 474.

Moreau, E., P. Lopez, P. Bauer, A. M. Tompkins, M. Janisková, and F. Chevallier, 2004: Variational retrieval of temperature and humidity profiles using rain rates versus microwave brightness temperatures, *Q. J. R. Meteorol. Soc.*, **130**, 827–852.

Ou, S. C. and K.-N. Liou, 1995: Ice microphysics and climate temperature feedback, *Atmos. Res.*, **35**, 127–138.

Platnick, S., M. D. King, S. A. Ackerman, W. P. Menzel, B. A. Baum, J. C. Riedi, and R. A. Frey, 2003: The MODIS Cloud Products: Algorithms and Examples from Terra, *itgrm*, **41**, 459–473.

Radnóti, G., Y. Trémolet, E. Andersson, L. Isaksen, E. Hólm, and M. Janisková, 2005: Diagnostics of linear and incremental approximations in 4D-Var revisited for higher resolution analysis, ECMWF Technical Memorandum No. 467.

Sharpe, M. C., 2006a: Incrementing cloud fractions, available from the author: martin.sharpe@metoffice.gov.uk.

Sharpe, M. C., 2006b: Incrementing grid–box cloud fraction and cloud liquid water content from PF model variables, available from the author: martin.sharpe@metoffice.gov.uk.

Sharpe, M. C., 2006c: An incrementing operator for both liquid and frozen cloud, available from the author: martin.sharpe@metoffice.gov.uk.

Slingo, 1989: A GCM parameterization for the shortwave radiative properties of water clouds, *J. Atmos. Sci.*, **46**, 1419–1427.

Stephens, G. L., D. G. Vane, R. Boain, G. G. Mace, K. Sassen, Z. Wang, A. J. Illingworth, E. J. O'Connor, W. Rossow, S. L. Durden, S. D. Miller, R. Austin, A. Benedetti, C. Mitrescu, and the CloudSat Science Team, 2002: The CloudSat mission and the A–train, *Bull. Amer. Meteor. Soc.*, **83**, 1771–1790.

Sun, J. and N. A. Crook, 1998: Dynamical and microphysical retrieval from Doppler radar observations using a cloud model and its adjoint. Part II: retrieval experiments of an observed Florida convective storm, *J. Atmos. Sci.*, **55**, 835–852.

Tompkins, A. M. and M. Janisková, 2004: A cloud scheme for data assimilation: Description and initial tests, *Q. J. R. Meteorol. Soc.*, **130**, 2495–2517.

Trémolet, Y., 2005: Incremental 4D–Var convergence study, ECMWF Technical Memorandum No. 469.

Tsuyuki, T., 1997: Variational data assimilation in the tropics using precipitation data. Part III: Assimilation of SSM/I precipitation rates, *Mon. Weather Rev.*, **125**, 1447–1464.

Vukićević, T., T. Greenwald, M. Županski, D. Županski, T. V. Haar, and A. S. Jones, 2004: Mesoscale cloud state estimation from visible and infrared satellite radiances, *Mon. Weather Rev.*, **132**, 3066–3077.

Wung, B., J. Verlinde, and J. Sun, 2000: Dynamical and microphysiscal retrievals from Doppler radar observations of a deep convective cloud, *J. Atmos. Sci.*, **57**, 262–283.

Županski, D. and F. Mesinger, 1995: Four-dimensional variational assimilation of precipitation data, *Mon. Wea. Rev.*, **123**, 1112–1127.